Ab Initio Study for Selective Oxidation of Methane with NO_x ($x = 1, 2$)

Yoichi Yamaguchi*

*Kansai Research Institute, Kyoto Research Park 17, Chudoji Minami-machi, Shimogyo-ku,
Kyoto 600-8813, Japan*

Yonghong Teng, Satoshi Shimomura, Kenji Tabata, and Eiji Suzuki

*Research Institute of Innovative Technology for the Earth, 9-2, Kizugawadai, Kizu-cho, Soraku-gun,
Kyoto 619-0292, Japan*

Received: March 22, 1999; In Final Form: August 20, 1999

A reaction model for the conversion of methane to C_1-oxygenates (methanol and formaldehyde) with NO_x ($x = 1, 2$) has been proposed theoretically using the ab initio molecular orbital method. The geometric and electronic structures for all the present molecules have been calculated by means of the MP2 (frozen core)/6-311++G(2d,p) level of theory. On the basis of the optimized structures, the single point calculations of the energies are carried out at the CCSD(T) level with the same basis sets. Through the theoretical analysis of the simplified CH_4-NO_x system instead of the experimental CH_4-O_2-NO system, we found the possible reaction path leading to C_1-oxygenates within all the barriers of less than 40 kcal/mol via CH_3O at 800 K. NO_2 has a higher activity for the hydrogen abstraction from methane than NO and O_2, though the calculated rate constants at 800 K indicate that this reaction is the rate-determining step in the conversion of methane to C_1-oxygenates. It is also found that increasing the concentration of NO promotes the yield of formaldehyde with the decreasing formation of methanol, which is consistent with recent experimental results in the CH_4-O_2-NO system.

I. Introduction

The selective oxidation of methane to C_1-oxygenates (methanol and formaldehyde) on metal−oxide catalysts has been the attractive subject of studies in recent years.[1] The conversion of a methane component of neutral gas to C_1-oxygenates is not only important for the petrochemical industry but also will be advantageous for safeguarding the environment.[2] Although a wide range of metal−oxide catalysts have been reported as active catalysts in reference to this subject, the products are mostly composed of CO, CO_2, and H_2O with only traces of CH_3OH, CH_2O, and C_2H_6. We have also studied this subject using $LiNbO_3$ and SnO_2 catalysts, aiming for a one-step reaction at a lower temperature (≈300−400 K) and pressure (1 atm) than the commercial process, and have detected components containing O^- that are similar to those of the other catalysts.[3−6] It has been confirmed that O^- works as a high active center for the hydrogen abstraction from methane on the metal−oxide catalysts[7−17] and also pointed out that the slow desorption of C_1-oxygenates from the surface of a catalyst brings about successive oxidation to yield CO and CO_2.[18,19] We have found theoretically that C_1-oxygenates are easily oxidized by O^- and their anionic species are stabilized on the SnO_2 catalyst, which lead to the difficulty of the desorption from the catalyst to the gas phase.[20]

On the other hand, the gas-phase reaction may be favorable to yielding C_1-oxygenates due to liberation from the above troubles, but the control of a chain reaction is generally difficult. For one of the approaches for the selective oxidation of methane in the gas phase, it has already been known that the oxidation of methane with O_2 is accelerated by the addition of NO,[21] which has been recently reconsidered by some groups.[22−24] Especially, Bañares et al.[25] have succeeded in the maximum yield, 7% of C_1-oxygenates at 883 K and 1 atm over V_2O_5/SiO_2 catalyst in CH_4-O_2-NO system. They have also suggested the important role of the gas-phase reactions (e.g., CH_4 + NO). Teng et al. have found for the first time that the maximum yield of C_1-oxygenates is close to 6% at 800 K and 1 atm in the noncatalytic CH_4-O_2-NO system.[26] In this system about 30% of NO is oxidized to NO_2 by O_2 under the equilibrium condition at 800 K,[27] though those researchers have not clarified enough the difference of the role of NO and NO_2. As far as we are aware, there is little experimental information on a detailed reaction mechanism for the conversion of methane to C_1-oxygenates with NO because of the difficulty of the analysis of the rapid consecutive radical chain reactions. A theoretical investigation has also not yet been conducted because this reaction system has many plausible pathways formed by a large number of elementary reactions with O_2.[28,29]

Therefore, we think that it is necessary to simplify the CH_4-O_2-NO system to the CH_4-NO_x ($x = 1, 2$) system and to clarify the difference of the role of NO and NO_2 in the former system through the present study on the latter system. We did not directly consider the role of coexistent oxygen for the formation of C_1-oxygenates, though it will be worthwhile to investigate a reaction path from methane to C_1-oxygenates in the simple system due to understanding the reaction mechanism in the CH_4-O_2-NO system.

In this paper, we theoretically investigate a possible pathway of the conversion of methane to C_1-oxygenates in the CH_4-NO_x ($x = 1, 2$) system. Our aim is different from the selective catalytic reduction of NO by methane with O_2 in the field of

---

* To whom correspondence should be addressed.

10.1021/jp990985a CCC: $18.00 © 1999 American Chemical Society
Published on Web 09/29/1999

SCHEME 1: Reaction Model for the Selective Oxidation of Methane with NO_x ($x = 1, 2$)

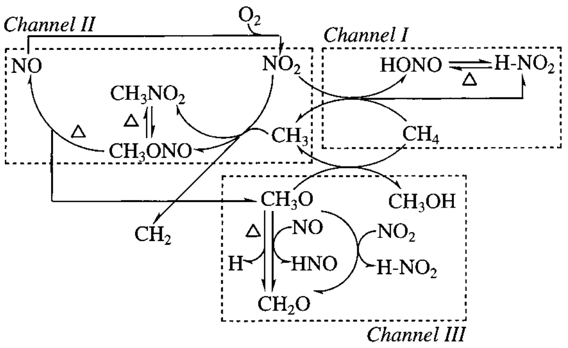

removal of NO_x from the exhausts of diesel and gasoline lean burn engines,[30,31] though our work may give useful information to the field.

II. Method of Calculation

All the calculations were carried out with the GAUSSIAN 94 ab initio program package.[32] The geometrical optimization for all the present molecules was performed with the MP2 (frozen core) level of theory and 6-311++G(2d,p) basis set. On the basis the optimized geometries, the single point calculations of the energies were carried out at the CCSD(T)/6-311++G(2d,p) level with the zero-point energy (ZPE) corrections of the MP2 level. All the optimized geometries corresponding to a local minimum point have real frequencies, except for a transition state with one imaginary frequency. Thermal rate constants for all the present elementary reactions at 800 K and 1 atm were also estimated using the calculated results of MP2 and CCSD(T) levels of theory. A Silicon Graphics Origin 2000 R10000 workstation was used for calculations in this study.

III. Results and Discussion

A. Reaction Channels for Selective Oxidation of Methane. Through the present theoretical calculations, we have proposed three reaction channels for the selective oxidation of methane in CH_4-NO_x system, as shown in Scheme 1. All the other elementary reactions with O_2, except for the oxidation of NO are omitted in Scheme 1. There is a lack of information on an active species in the CH_4-O_2-NO system, though it is expected that the initial reaction step is the abstraction of a hydrogen atom from CH_4 with NO_x (or O_2) and a formation of CH_3. As mentioned above, our main concern is to clarify the difference of the role of NO and NO_2 through the examination of a reaction path for the formation of C_1-oxygenates in the CH_4-NO_x system.

Channel I shows the reactions of the hydrogen abstraction from CH_4 with NO_2. Next, channel II shows the hydrogen abstraction from CH_3 with NO_2, the radical couplings of CH_3 with NO_2 and the formation of CH_3O. Last, channel III shows the reactions for the formation of C_1-oxygenates via CH_3O, which are the most important reactions for the conversion of methane. In channel III we found one and three possible reaction pathways to yield CH_3OH and CH_2O, respectively. We will explain channels I−III in details below, though we would like to examine a little of the CH_4 + NO reaction for comparison with the activity for the hydrogen abstraction from CH_4 with NO_2 (or O_2). This reaction has not yet been conducted enough theoretically.

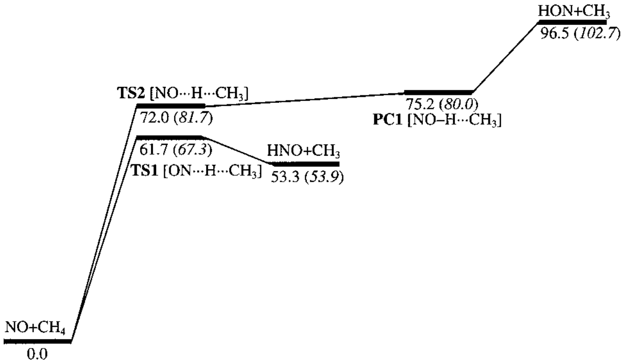

Figure 1. Potential energy diagram for the NO + CH_4 reaction. The total energy for the separated reactants NO + CH_4 is −170.0343 (−169.9861) hartrees. Values in parentheses represent MP2 level of calculations. Relative energies are given in kcal/mol.

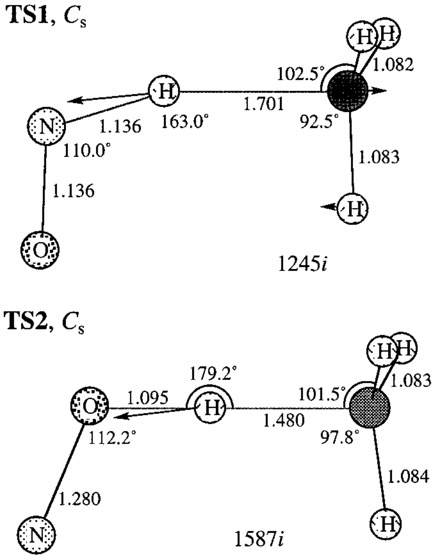

Figure 2. Optimized geometries for TS1 and TS2 of the NO + CH_4 reaction. All bond lengths and bond angles are given in Å and degrees, respectively. Imaginary frequency modes for the forward reactions are given in cm^{-1}.

B. Reaction of CH_4 with NO. The elementary reactions for the abstraction hydrogen from CH_4 with NO are

$$NO + CH_4 \rightarrow [TS1] \rightarrow HNO + CH_3 \qquad (1)$$

$$NO + CH_4 \rightarrow [TS2] \rightarrow [PC1] \rightarrow HON + CH_3 \qquad (2)$$

The potential energy diagram for eqs 1 and 2 is illustrated in Figure 1; here the total energy of CH_4 + NO is taken as a standard. MP2 energies with ZPE corrections were also shown in parentheses in all the odd-numbered figures for comparison. We checked by the bond dissociation energy of $H-CH_3$ whether the calculated value, 99.5 kcal/mol, compares well with the experimental one, 104 kcal/mol, but the error is about 5 kcal/mol. The optimized geometries of transition states TS1 and TS2 with the C_s structures are illustrated in Figure 2. The optimized geometry of the product complex, PC1, is omitted in Figure 2, though the O−H and H(O)−C bond lengths of PC1 are 0.99 and 2.11 Å, respectively. The transition vectors leading to the forward reactions and the corresponding imaginary frequencies for TS1 and TS2 are also shown in Figure 2. In TS1 and TS2 the transition vectors are almost located at a mode related to the abstracted hydrogen atoms for TS1 and TS2, and the transition states have near-collinear N (or O)−H−C geometries.

TABLE 1: Atomic Net Charges and Atomic Spin Densities for TS1 and TS2 of the $CH_4 + NO$ Reaction

		$CH_4 + NO$	TS1 $[H_3C\cdots H_a\cdots NO]$	TS2 $[H_3C\cdots H_a\cdots ON]$
atomic net charges	N	0.00	−0.12	−0.10
	O	0.00	−0.09	−0.33
	H_a	+0.12	+0.28	+0.48
	C	−0.48	−0.51	−0.55
atomic spin densities	N	+0.90	+0.45	+1.89
	O	+0.10	−0.16	−0.20
	H_a	0.00	−0.20	+0.17
	C	0.00	+1.13	−1.05

It can be seen in Figure 2 that the C−H bond length of TS1 is longer than that of TS2, indicating that the barrier of eq 1 is located near the product end of the reaction.

The atomic net charges and atomic spin densities for TS1 and TS2 are summarized in Table 1. A separated NO has no charge polarization, and its spin is almost localized at the nitrogen atom. The $O-H_a$ bond of TS2 has a larger charge polarization than the $N-H_a$ bond of TS1, indicating that the electronic structure of TS2 has a slightly charge-transfer nature in comparison with that of TS1. On the other hand, the former has a smaller spin polarization than the latter.

In Figure 1 the transition barriers for eq 1 are 61.7 kcal/mol for the forward reaction and 8.4 kcal/mol for the backward one. In the case of eq 2 we find a higher barrier of 72.0 kcal/mol for the forward reaction (compared with eq 1) and a lower barrier for the backward one via PC1, where TS2 is more stabilized than PC1, though we think that the energy difference between them is very sensitive to the level of theory, especially the electron correlation. The nitrogen atom of NO has a slightly higher activity for the hydrogen abstraction from CH_4 than the oxygen atom of NO. In both eqs 1 and 2 the backward reactions are more favorable than the forward ones, though the forward reactions may be rather promoted because the products, HNO (or HON), will be easily oxidized by oxygen in the CH_4-O_2-NO system. Considering the very slow $O_2 + CH_4 \rightarrow O_2H + CH_3$ reaction at 800−900 K,[26] whose barrier is 59.0 kcal/mol in the same level of theory,[33] eqs 1 and 2 can be almost never promoted within the range of the above temperature. Therefore, it is assumed that both O_2 and NO are not the active species for the reaction of the hydrogen abstraction from CH_4 in the CH_4-O_2-NO system.

C. Reaction of CH_4 with NO_2. Next we consider the elementary reactions in channel I:

$$NO_2 + CH_4 \rightarrow [TS3] \rightarrow H-NO_2 + CH_3 \tag{3}$$

$$NO_2 + CH_4 \rightarrow [TS4] \rightarrow trans\text{-}HONO + CH_3 \tag{4}$$

$$H-NO_2 \rightarrow [TS5] \rightarrow trans\text{-}HONO \tag{5}$$

As mentioned previously, NO_2 is formed by the oxidation of NO in the CH_4-O_2-NO system. The potential energy diagram for eqs 3 and 4 is illustrated in Figure 3; here the total energy of $CH_4 + NO_2$ is taken as a standard. The optimized geometries of transition states TS3 and TS4 with the C_1 structures and TS5 with the C_s structure are illustrated in Figure 4. TS5 is a transition state of the thermal isomerization of $H-NO_2$ to nitrous acid, *trans*-HONO. In TS3 and TS4 the transition vectors are located at a mode related to the abstracted hydrogen atoms, and these transition states have near-collinear N (or O)−H−C geometries, such as TS1 and TS2. The C−H bond lengths of TS3 and TS4 are shorter than those of TS1 and TS2, indicating that the barriers of eqs 3 and 4 are located nearer to the reactant end of the reaction in comparison with those of eqs 1 and 2.

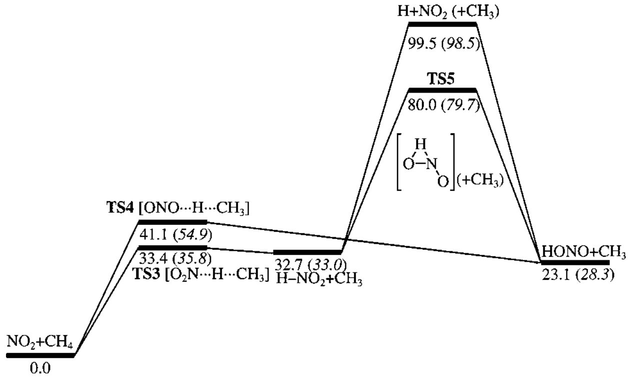

Figure 3. Potential energy diagram for channel I. The total energy for the separated reactants $NO_2 + CH_4$ is −245.0879 (−245.0432) hartrees. Values in parentheses represent MP2 level of calculations. Relative energies are given in kcal/mol.

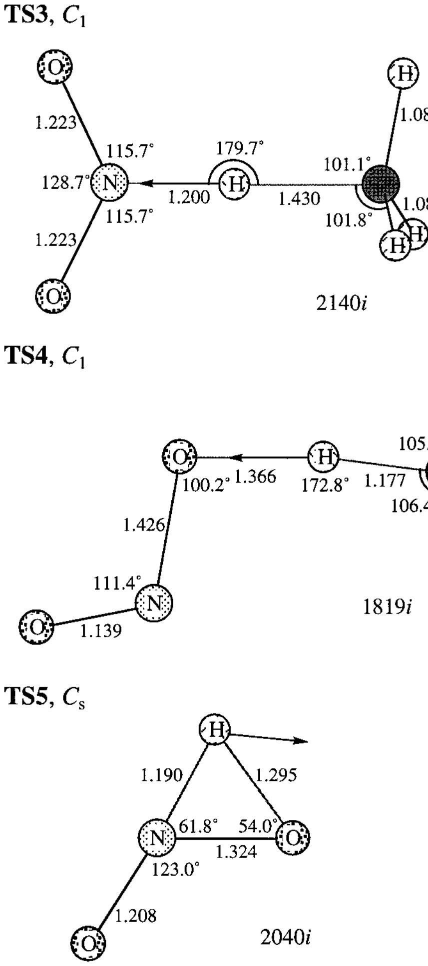

Figure 4. Optimized geometries for TS3 and TS4 of the $NO_2 + CH_4$ reaction and TS5 of the thermal isomerization of HNO_2.

The atomic net charges and atomic spin densities of TS3 and TS4 are also summarized in Table 2. The O_a-H_a bond of TS4 has a large spin polarization in contrast to TS2. On the other hand the electronic structure of TS3 has a charge-transfer nature due to having a large net charge on the O_a-H_a bond, such as TS2. Therefore, the transition states in Tables 1 and 2 have significantly different charge and spin distributions whether the nitrogen atom of NO_2 or the oxygen atom of NO_2 attacks a hydrogen atom of CH_4.

In Figure 3 the transition barriers for eq 3 are 33.4 kcal/mol for the forward reaction and only 0.7 kcal/mol for the backward

TABLE 2: Atomic Net Charges and Atomic Spin Densities for TS3 and TS4 of the $CH_4 + NO_2$ Reaction

		$CH_4 + NO_2$	TS3 $[H_3C \cdots H_a \cdots N(O_a)_2]$	TS4 $[H_3C \cdots H_a \cdots O_aNO_b]$
atomic net charges	N	+0.26	−0.02	+0.04
	O_a	−0.13	−0.21	−0.11
	O_b			−0.03
	H_a	+0.12	+0.47	+0.27
	C	−0.48	−0.54	−0.59
atomic spin densities	N	+0.50	+0.30	+0.07
	O_a	+0.25	+0.03	+0.92
	O_b			−0.16
	H_a	0.00	−0.15	−0.16
	C	0.00	+0.97	+0.40

one. The latter barrier has a very small value, which may be affected by the level of theory, such as mentioned in eq 2. Equation 4 has a higher barrier of 41.1 kcal/mol for the forward reaction compared with that of eq 3 and a barrier of 18.0 kcal/mol for the backward one. Thus, the backward reaction of eq 3 is energetically easier than that of eq 4. But we think that the forward reactions in both eqs 3 and 4 are promoted in the CH_4-O_2-NO system because the products, $H-NO_2$ (or HONO), will be easily oxidized by oxygen. The nitrogen atom of NO_2 has a higher activity for the hydrogen abstraction from CH_4 than the oxygen atoms of NO_2, such as in the case of the $CH_4 + NO$ reaction. The energy difference between TS3 and TS4, 7.7 kcal/mol, is smaller than that of TS1 and TS2, 10.3 kcal/mol, indicating a somewhat high activity of the oxygen atoms in NO_2 because of the large spin density of the atoms in NO_2 in comparison with that in NO. The barriers for the forward reactions in eqs 3 and 4 are significantly lower by about 30 kcal/mol than those in eqs 1 and 2 and also lower by about 20−25 kcal/mol than the $O_2 + CH_4 \rightarrow O_2H + CH_3$ reaction. The calculated rate constants and activation energies at 800 K are summarized in Table 3. The data were calculated by using the conventional transition-state theory. The rate constants for eqs 3 and 4 show larger values than those of eqs 1 and 2 and the $O_2 + CH_4 \rightarrow O_2H + CH_3$ reaction. Therefore, we found that the initial reaction step, namely the hydrogen abstraction from CH_4, is caused by NO_2 rather than NO and O_2. It is assumed that this situation is the same as in the case of the CH_4-O_2-NO system despite a low concentration of NO_2.

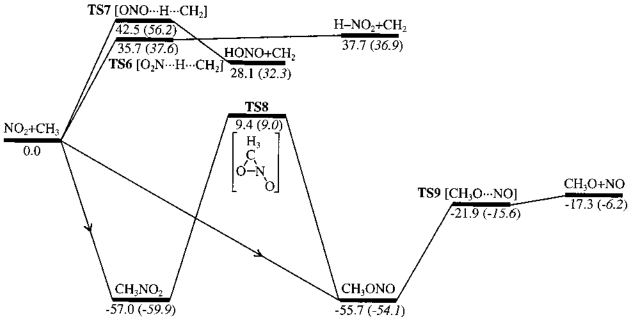

Figure 5. Potential energy diagram for channel II. The total energy for the separated reactants $NO_2 + CH_3$ is −244.4295 (−244.3864) hartrees. Values in parentheses represent MP2 level of calculations. Relative energies are given in kcal/mol.

It can be seen in Figure 3 that eq 5 has a lower barrier of 47.3 kcal/mol for the forward reaction compared with that of 56.9 kcal/mol for the backward one. These barriers are lower than the energy for the thermal decomposition of $H-NO_2$ (or HONO) to a hydrogen atom and NO_2. Thus, it is expected that $H-NO_2$ is a stable species as well as HONO, though the former is a rare chemical species. As mentioned above, we think that the $H-NO_2 + O_2 \rightarrow NO_2 + O_2H$ reaction may occur in the CH_4-O_2-NO system. Next, we investigated the further reaction, $NO_2 + CH_3$, in detail below.

D. Reaction of CH_3 with NO_2. We consider four possible elementary reactions in channel II:

$$NO_2 + CH_3 \rightarrow [TS6] \rightarrow H-NO_2 + CH_2 \tag{6}$$

$$NO_2 + CH_3 \rightarrow [TS7] \rightarrow \textit{trans}\text{-HONO} + CH_2 \tag{7}$$

$$CH_3NO_2 \rightarrow [TS8] \rightarrow \textit{trans}\text{-}CH_3ONO \tag{8}$$

$$\textit{trans}\text{-}CH_3ONO \rightarrow [TS9] \rightarrow CH_3O + NO \tag{9}$$

Equations 6 and 7 represent the reactions of the hydrogen abstraction from CH_3. The radical coupling of CH_3 with NO_2 can directly produce nitromethane, CH_3NO_2 and methylnitrite, *trans*-CH_3ONO (see Figure 5). Equation 8 represents the reaction of the thermal isomerization from CH_3NO_2 to CH_3ONO. Equation 9 is the thermal decomposition of CH_3ONO, which is the most important reaction because only CH_3O can lead to C_1-oxygenates, as seen in Scheme 1.

The potential energy diagram for eqs 6−9 is illustrated in Figure 5; here the total energy of $CH_3 + NO_2$ is taken as a standard. The optimized geometries of TS6, TS7, and TS9 with the C_s structures and TS8 with the C_1 structure are illustrated

TABLE 3: Calculated Rate Constants, *k*, and Activation Energies, E_A, at 800 K[a]

reaction	*k*	E_A (kcal/mol)
channel I		
$CH_4 + NO_2 \rightarrow CH_3 + H\text{-}NO_2$	5.4×10^{-20}	37.6
$CH_4 + NO_2 \rightarrow CH_3 + \textit{trans}\text{-HONO}$	3.3×10^{-22}	45.8
channel II		
$CH_4 + NO_2 \rightarrow CH_2 + H\text{-}NO_2$	1.2×10^{-21}	39.6
$CH_3 + NO_2 \rightarrow CH_2 + \textit{trans}\text{-HONO}$	5.1×10^{-23}	46.9
$CH_3NO_2 \rightarrow \textit{trans}\text{-}CH_3ONO$	2.8×10^{-6} (1.4×10^{-4})	67.9 (67.0)
rans-$CH_3ONO \rightarrow CH_3O + NO$	2.5×10^{5}	35.6
channel III		
$CH_3O + CH_4 \rightarrow CH_3OH + CH_3$	1.8×10^{-15} (9.9×10^{-16})	16.9 (11.0)
$CH_3O \rightarrow CH_2O + H$	2.2×10^{6} (6.4×10^{5})	27.5 (30.0)
$CH_3O + NO_2 \rightarrow CH_2O + HNO_2$	1.1×10^{-15}	6.7
$CH_3O + NO_2 \rightarrow CH_2O + HNO$	3.1×10^{-14} (2.6×10^{-12})	5.6 (−0.4)
other reactions		
$CH_4 + NO \rightarrow CH_3 + HNO$	1.4×10^{-27}	65.6
$CH_4O + NO \rightarrow CH_3 + HON$	4.3×10^{-30}	76.3
$CH_4 + O_2 \rightarrow CH_3 + HO_2$[b]	1.0×10^{-26} (1.9×10^{-26})	59.0 (56.9)

[a] Values in parentheses represent the experimental data taken from refs 28 and 29. Rate constants are in s^{-1} and cm^3 $molecule^{-1}$ s^{-1} for unimolecular and bimolecular reactions, respectively. Activation energies are in kcal/mol. [b] From ref 33.

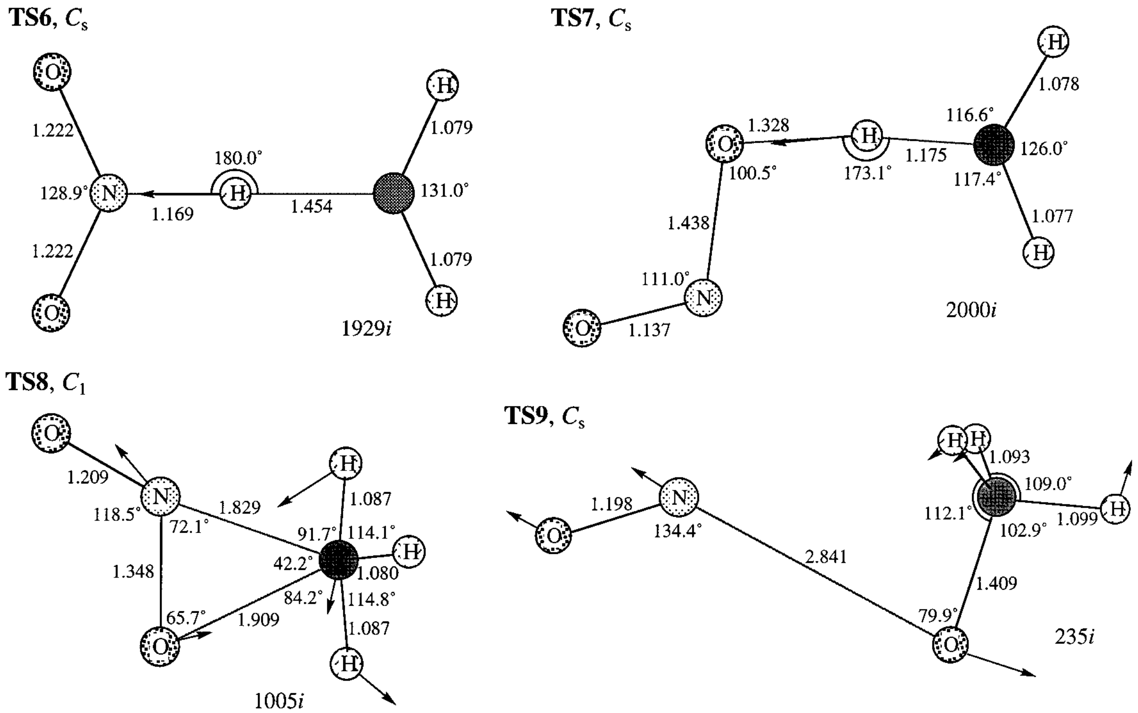

Figure 6. Optimized geometries for TS6 and TS7 of the $NO_2 + CH_3$ reaction, TS8 of the thermal isomerization of CH_3NO_2, and TS9 of the thermal decomposition of *trans*-CH_3ONO.

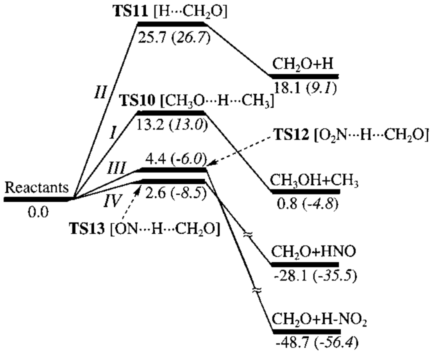

Figure 7. Potential energy diagram for channel III. The total energies for the separated reactants $CH_3O + CH_4$ (I), CH_3O (II), $CH_3O + NO_2$ (III), and $CH_3O + NO$ (IV) are −155.1623 (−155.0957) hartrees, −114.7925 (−114.7529) hartrees, −319.5106 (−319.4534) hartree, and −244.4570 (−244.3963) hartrees, respectively. Values in parentheses represent MP2 level of calculations. Relative energies are given in kcal/mol.

in Figure 6. We find that TS6 and TS7 have structures similar to those of TS3 and TS4, respectively. The transition vectors are located at a mode related to the abstracted hydrogen atoms for TS6 and TS7, and the transition states have near-collinear N (or O)−H−C geometries.

In Figure 5 the transition barriers for eqs 6 and 7 are 35.7 and 42.5 kcal/mol, respectively, which are similar values to those for eqs 3 and 4. In eq 6 the products are unstable as compared to TS6 because they may also be affected by the level of theory. We find in Table 3 that the rate constants of eqs 6 and 7 have values one digit smaller than those of eqs 3 and 4. Further reactions of CH_2 with NO_2 will occur one after another until yielding carbon atom, which leads to yield CO and CO_2. Also in eqs 6 and 7 the nitrogen atom of NO_2 has a higher activity than the oxygen atom, such as in eqs 3 and 4. Although in Figure 5 the thermal decomposition of CH_3NO_2 (or CH_3ONO) to NO_2 and CH_3 is more energetically favorable than eq 8, it is difficult to promote these reactions at 800 K because of their significantly high barriers in comparison with the barrier of eq 3. Thus, CH_3NO_2 is a stable species in the present system. On the other hand CH_3ONO is easily decomposed to CH_3O and NO via TS9 whose barrier at 800 K is similar to the barrier of eq 3. Bañares et al.[25] have not reported on the formation of CH_3NO_2, though we have found that the injected NO is almost changed to CH_3NO_2 at 800 K in the CH_4−O_2−NO system.[26] Our experimental result supports the present study. We found in Table 3 that there is a possible reaction path from the initial reaction step of eq 3 to yield CH_3O and NO via CH_3ONO with energies of less than 40 kcal/mol at 800 K. We think that the $O_2 + CH_3 \rightarrow CH_3OO$ reaction has also to be considered in the case of the CH_4−O_2−NO system. But a theoretical approach will be conducted with a very limited set of elementary reactions because of the large number of additional consecutive reactions with O_2 and/or NO_x, which needs more detailed experimental analysis and will be published elsewhere.[34]

E. Production of C_1-Oxygenates. The elementary reactions for the formation of C_1-oxygenates in channel III are

$$CH_4 + CH_3O \rightarrow [TS10] \rightarrow CH_3 + CH_3OH \quad (10)$$

$$CH_3O \rightarrow [TS11] \rightarrow H + CH_2O \quad (11)$$

$$NO_2 + CH_3O \rightarrow [TS12] \rightarrow H{-}NO_2 + CH_2O \quad (12)$$

$$NO + CH_3O \rightarrow [TS13] \rightarrow H{-}NO + CH_2O \quad (13)$$

Equation 10 can only lead to the formation of CH_3OH, the others lead to CH_2O. The potential energy diagram for eqs 10−13 is illustrated in Figure 7; here the total energy of each separated reactant is taken as a standard. The optimized geometries of transition states TS10 and TS11 with the C_s structures and TS12 and TS13 with the C_1 structures are illustrated in Figure 8. The transition barrier for eq 10 is 13.2 kcal/mol for the forward reaction. The thermal decomposition of CH_3O to CH_2O in eq 11 has a higher barrier of 25.7 kcal/mol than eq 10. On the other hand, eqs 12 and 13 have significantly low barriers of

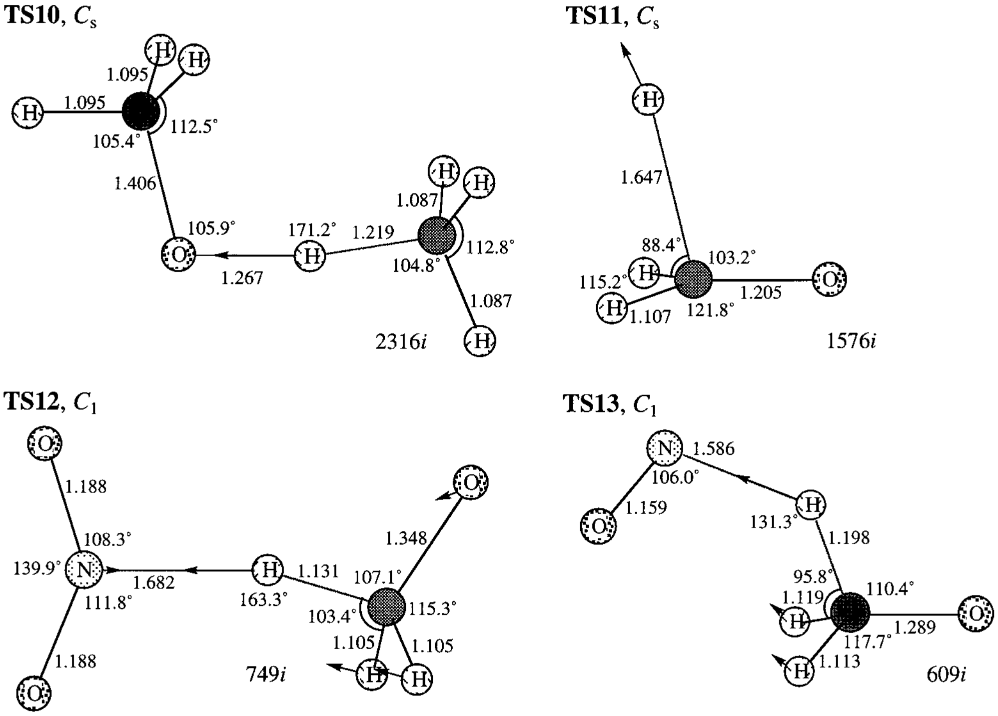

Figure 8. Optimized geometries for TS10 of the $CH_3O + CH_4$ reaction, TS11 of the thermal decomposition of CH_3O, TS12 of the $CH_3O + NO_2$ reaction, and TS13 of the $CH_3O + NO$ reaction.

4.4 and 2.6 kcal/mol, respectively, where NO is formed by the thermal decomposition of CH_3ONO in eq 9. Although NO has a very low activity for the hydrogen abstraction from CH_4 compared with NO_2, it can be seen in Table 3 that NO has a slightly higher activity for the hydrogen abstraction from CH_3O than NO_2. Especially, the rate constant for eq 13 is one digit larger in theory and four digits larger in experiment than that for eq 10, indicating that NO is an important species that affects the production ratio of CH_3OH to CH_2O. Thus, it is expected that increasing the concentration of NO promotes the yield of CH_2O with decreasing formation of CH_3OH, which is consistent with our recent experimental results.[26] In Table 3 we notice that the hydrogen abstraction from CH_4 with NO_2 in eq 4 is the rate-determining step for the conversion of CH_4 to C_1-oxygenates. Therefore, we found a possible reaction pathway for the conversion of CH_4 to C_1-oxygenates in the CH_4-NO_x system within all the barriers of less than 40 kcal/mol at 800 K.

IV. Conclusions

We have proposed theoretically a reaction model of the conversion of methane to C_1-oxygenates with NO_x ($x = 1, 2$) in the gas phase. We have applied the MP2 (frozen core) and CCSD(T) levels of theory with the 6-311++G(2d,p) basis set. We found a possible reaction path for the formation of C_1-oxygenates within all the barriers of less than 40 kcal/mol via CH_3O at 800 K. NO_2 has a higher activity for the cleavage of the C$-$H bond of methane than NO and O_2, which is the rate-determining step at 800 K in the CH_4-NO_x system. Increasing the concentration of NO promotes the yield of CH_2O with the decreasing formation of CH_3OH, which is consistent with recent experimental results in the CH_4-O_2-NO system. We have investigated the reaction pathway for the conversion of methane to C_1-oxygenates in the simplified CH_4-NO_x system, though we believe that this study will be helpful for understanding the reaction mechanism in the CH_4-O_2-NO system.

Acknowledgment. This work was partially supported by the New Energy and Industrial Technology Development Organization (NEDO) Environmental Catalyst Research Project.

References and Notes

(1) See for instance: Krylov, O. V. *Catal. Today* **1993**, *18*, 209 and references therein.

(2) Firor, F. *The Changing Atmosphere*; Yale University Press: New Haven, CT, 1990; p 52.

(3) Tabata, K.; Choso, T. *Appl. Surf. Sci.* **1998**, *134*, 139.

(4) Choso, T.; Tabata, K. *J. Mol. Catal.* **1998**, *A129*, 225.

(5) Nagasawa, Y.; Choso, T.; Karasuda, T.; Shimomura, S.; Ouyang, F.; Tabata, K.; Yamaguchi, Y. *Surf. Sci.*, in press.

(6) Kawabe, T.; Tabata, K.; Nagasawa, Y.; Yamaguchi, Y. *Surf. Sci.*, in press.

(7) See for instance: Mehandru, S. P.; Anderson, A. B.; Brazdil, J. F. *J. Am. Chem. Soc.* **1988**, *110*, 1715.

(8) Goto, A.; K. Aika, K. *Bull. Chem. Soc. Jpn.* **1998**, *71*, 95.

(9) Driscoll, D. J.; W. Martir, W.; Wang, J. X.; Lunsford, J. H. *J. Am. Chem. Soc.* **1985**, *107*, 58.

(10) Au, C. T.; Roberts, M. W. *J. Chem. Soc., Faraday Trans. I* **1987**, *83*, 2047.

(11) Hutchings, G. J.; Scurrell, M. S.; Woodhouse, J. R. *J. Chem. Soc., Chem. Commun.* **1987**, 1388.

(12) Anpo, M.; Sunamoto, M.; Doi, T.; Matsuura, I. *Chem. Lett.* **1988**, 701.

(13) Cant, N. W.; Lukey, C. A.; Nelson, P. F.; Tyler, R. J. *J. Chem. Soc., Chem. Commun.* **1988**, 766.

(14) Mehandru, S. P.; Anderson, A. B.; Brazdil, J. F.; Grasselli, R. K. *J. Phys. Chem.* **1987**, *91*, 2930.

(15) Børve, K. J.; Pettersson, L. G. M. *J. Phys. Chem.* **1991**, *95*, 7401.

(16) Børve, K. J. *J. Chem. Phys.* **1991**, *95*, 4626.

(17) Yamaguchi, Y.; Nagasawa, Y.; Murakami, A.; Tabata, K. *Int. J. Quantum Chem.* **1998**, *69*, 669.

(18) Pak, S; Rosynek, M. P.; Lunsford, J. H. *J. Phys. Chem.* **1994**, *98*, 11786.

(19) Taylor, S. H.; Hargreves, J. S. J.; Hutchings, G. J.; Joyner, R. W. In *Methane and Alkane Conversion Chemistry*; Bhasin, M. M., Slocum, D. W., Eds.; Plenum Press: New York, 1995; p 339.

(20) Yamaguchi, Y.; Nagasawa, Y.; Shimomura, S.; Tabata, K. *Int. J. Quantum Chem.*, in press.

(21) Layng, T. E.; Soukop, R. *Ind. Eng. Chem.* **1928**, *20*, 1052.

(22) Irusta, S.; Lombardo, E. A.; EMiró, E. E. *Catal. Lett.* **1994**, *29*, 339.

(23) Han, L. B.; Tsubota, S.; Haruta, M. *Chem. Lett.* **1995**, 931.

(24) Otsuka, K.; Takahashi, R.; Amakawa, K.; Yamanaka, T. *Catal. Today*. **1998**, *45*, 23.

(25) Bañares, M. A.; Cardoso, J. H.; Hutchings, G. J.; Bueno, J. M. C.; Fierro, J. L. G. *Catal. Lett.* **1998**, *56*, 149.

(26) Teng, Y.; Sakurai, H.; Tabata, K.; Suzuki, E. *Appl. Catal*., in press.

(27) Estimated by Modell, M.; Reid, R. C. *Thermodynamics and its Applications*; Prentice-Hall: Englewood Cliffs, NJ, 1974; p 396.

(28) Arutyunov, V. S.; Basevich, V. Y.; Vedeneev, V. I. *Russ. Chem. Rev.* **1996**, *65*, 197.

(29) Bromly, J. H.; Barnes, F. J.; Muris, S.; You, X.; Haynes, B. S. *Combust. Sci. Technol.* **1996**, *115*, 259.

(30) Sasaki, M.; Hamada, H.; Kintaichi, Y.; Itoh, T. *Catal. Lett.* **1991**, *11*, 177.

(31) Witzel, F.; Sill, G. A.; Hall, W. K. *J. Catal.* **1994**, *149*, 229.

(32) Frisch, M. J.; Trucks, G. W.; Schlegel, H. B.; Gill, P. M. W.; Johnson, B. G.; Robb, M. A.; Cheeseman, J. R.; Keith, T. A.; Patterson, G. A.; Montgomery, J. A.; Raghavachari, K.; Al-Laham, M. A.; Zakrzewski, V. G.; Ortiz, J. V.; Foresman, J. B.; Cioslowski, J.; Stefanov, B. B.; Nanayakkara, A.; Challacombe, M.; Peng, C. Y.; Ayala, P. Y.; Chen, W.; Wong, M. W.; Andres, J. L.; Replogle, E. S.; Gomperts, R.; Martin, R. L.; Fox, D. J.; Binkley, J. S.; Defrees, D. J.; Baker, J.; Stewart, J. J. P.; Head-Gordon, M.; Gonzalez, C.; Pople, J. A. *Gaussian 94;* Gaussian, Inc.: Pittsburgh, PA, 1995.

(33) Yamaguchi, Y. Unpublished results.

(34) Tabata, K.; Teng, Y.; Yamaguchi, Y.; Sakurai, H.; Suzuki, E. *J. Phys. Chem.*, submitted.